AIMS Mathematics, 10(5): 12598–12618.
DOI: 10.3934/math.2025568
Received: 16 March 2025
Revised: 19 May 2025
Accepted: 23 May 2025
Published: 29 May 2025

https://www.aimspress.com/journal/Math

Research article

A food chain model with Allee effect: Analysis on the behaviors of equilibria

Huda Abdul Satar[1], Raid Kamel Naji[1,2,*] and Mainul Haque[3]

[1] Department of Mathematics, College of Science, University of Baghdad, Baghdad, Iraq
[2] Scientific Research Commission, Baghdad, Iraq
[3] School of Mathematical Science, The University of Nottingham Ningbo China, Ningbo, China

* **Correspondence:** Email: raid.naji@sc.uobaghdad.edu.iq.

Abstract: The Allee effect is crucial to population ecology and conservation biology because it clarifies how difficult it can be for tiny populations to endure and expand. Low population densities make it more difficult for individuals to survive or reproduce in a phenomenon. Therefore, it is important to study the ecological system, including the Allee effect. Accordingly, our goal in this paper was to examine equilibria's behaviors in a three-species food chain model incorporating the Allee effect. This model includes a linear type of functional response. The points of equilibrium are categorized and depicted. The behaviors of these equilibrium points are then illustrated analytically through stability and bifurcation analyses. Moreover, the numerical simulation utilizes realistic hypothetical data to confirm the analytical results and detect the influence of varying the parameters on the system's dynamics. It is observed that the system undergoes bistable behavior; otherwise, the trivial equilibrium point is globally asymptotically stable. Under specific circumstances, the food chain system experiences a transcritical bifurcation around the axial and border equilibrium points. However, under some conditions, a Hopf bifurcation happens around the border equilibrium point.

Keywords: Allee effect; food chain; stability; bifurcation
Mathematics Subject Classification: 92D25, 34L30, 92D40

1. Introduction

A tri-trophic system with prey, a predator, and an apex predator is frequently used to illustrate a

food chain model, which usually consists of several creatures dependent on one another for sustenance. Ecosystem stability and interactions are studied using this structure. The system's stability and dynamics are impacted by the many functional responses employed to describe the interactions between species, such as predator-dependent [8], ratio-dependent [13], and prey-dependent [4,12,20] interactions. Food chain models, commonly used in applied mathematics and theoretical ecology, include prey, predators, and superpredators. Some self-interaction linkages between various trophic levels were discovered in prior investigations. Gakkhar and Naji [9] examined a three-trophic-level food chain model with ratio-dependent predation for the interaction. They showed this model's stability, periodicity, and chaotic dynamics under a range of biologically realistic parameter values. Later research has created and examined other food chain models that use ratio-dependent functional responses; see [1,2,14]. They demonstrated that these food chain systems can produce a variety of dynamic behaviors, including chaotic dynamics.

Pathak et al. [24] introduced a three-level food chain model with a Hassle-Varley functional response to investigate the dynamic behavior and the effect of discrete time delays on the system's stability. Similar results have been found in most studies of continuous-time deterministic models, pointing to two basic patterns: An approach to equilibrium or a limit cycle; for example, see [6,19,22,29] and the references therein. The implicit assumption that the majority of food chains in nature match a stable equilibrium in the model served as the basic rationale for such an analysis. A tri-trophic food chain model was examined by Pattanayak et al. [25] using conventional techniques as a substitute for local stability analysis, utilizing perspective basin stability analysis. For multistable ecosystems, especially for specific transitions between two different stable states, basin stability analysis is more suitable. Over a broad range of parameters, they found that a food chain model transitions from monostability to bistability and vice versa. Tanner [30] examined eight food chain systems that account for the natural population growth rate of prey and their predators using numerical simulation and analytical analysis. Upadhyay and Naji [31] studied a three-trophic-level food chain model with a hybrid type of predator- and prey-dependent functional response. Once persistence conditions were established, it analyzed local and global stability and generated bifurcation diagrams with biologically feasible values. Furthermore, this study illustrated the basic steps and methods of biological food chain analysis. The obtained data illustrated the many complex features of the system, such as periodic, chaotic, and stable dynamics. Subsequent research on the dynamics of three-species food chain models revealed intricate dynamics, such as chaos; see, for instance, [7,17,23,34]. Moreover, understanding real-world ecological systems requires an understanding of complex dynamics, such as oscillations and bifurcations, which can result from the introduction of extra elements like refuges [10,33], illness [5,28], predator cannibalism [18], and fear [15]. Recently, there has been consideration of a diffusive predator-prey model that incorporates the fear effect and nonlocal competition [35].

Allee first coined the phrase "Allee effect" in 1931. It describes a process that slows down a population's increase at low densities and frequently happens in fisheries, plants, vertebrates, and invertebrates. This phenomenon is sometimes referred to as the dispensation effect in fisheries and the negative competition impact on population dynamics. In a given species, the Allee effect often denotes a positive relationship between any aspect of individual fitness and population density. Numerous environmental conditions, such as low-density mating partner difficulty, genetic inbreeding, social felicitation of reproduction, low mating probability, depletion of the inbreeding rate, and antipredator aggression, might contribute to the Allee effect [3,32]. Consequently, by slowing growth rates at low population densities, the Allee effect can majorly affect population

dynamics and even cause extinction [16, 21]. In models, the Allee effect is frequently a bifurcation parameter that affects equilibrium stability and causes phenomena like Hopf bifurcations. While moderate Allee intensity can stabilize populations by lowering chaotic oscillations, high Allee intensity can hinder species' cohabitation [27]. Under some circumstances, the Allee effect can stabilize populations even though it can cause a population's decrease and extinction. The Allee effect and the food chain model interact to show how complicated ecological systems are and how variables like more food and fear can further affect the results, providing insights on preserving ecological balance and biodiversity.

Based on the findings above, the interest in studying simple food chains when there is an Allee effect is increasing because of its impact on the existence and persistence of living organisms in the environment, which is the main contribution of this study. The need to get a deeper understanding of intricate ecological dynamics and the relationships among population growth, predation, and survival thresholds is the motivation for studying a food chain model with the Allee effect, with a special emphasis on equilibrium behaviors. Accordingly, this research is carried out by proposing and studying a novel trigeneric food chain involving an Allee effect. The purpose is to discover the role of the Allee effect on the dynamics of a simple food chain. The structure of the paper is as follows: In Section 2, the mathematical model is developed. The stability and bifurcation evaluations of the developed model are carried out in Section 3. In Section 4, a numerical simulation is presented. The results obtained are discussed in Section 5. Section 6 presents the conclusion.

2. Model formulation

A three-trophic-level food chain model, which includes the prey, a predator, and a superpredator, is examined in this work. The model uses the following system of ordinary differential equations (ODEs) to represent a specific Allee effect manifestation:

$$\begin{aligned} \frac{dx}{dt} &= rx\left(1-\frac{x}{k}\right)\left(1-\frac{n_1+n_2}{x+n_2}\right)-m_1xy, \\ \frac{dy}{dt} &= e_1m_1xy-m_2yz-d_1y, \\ \frac{dz}{dt} &= e_2m_2yz-d_2z. \end{aligned} \tag{1}$$

The model system has a Lotka-Volterra (or Holling Type I) functional response (1). The premise behind the Lotka-Volterra functional response is that predator feeding rates rise linearly with the density of their prey population. Furthermore, the prey density, predator density, and superpredator density at time t are represented by the variables $x(t)$, $y(t)$, and $z(t)$, respectively. The positive constants defined by the parameters r, k, m_i, e_i, d_i, and n_i correspond to the following: the prey's intrinsic growth rate, environmental carrying capacity, consumption rates, conversion rates, species death rates, and Allee constants, respectively. By looking at this model system, we can determine the basic relationship between these three levels: y only preys on x, and z exclusively preys on y. This approach does not consider nutrient recycling.

We initially disregard the Allee effect by leaving out the Allee constants to derive this food chain model without the Allee impact. The three-trophic-level food chain model with the Lotka-Volterra functional response can be as follows:

$$\frac{dx}{dt} = rx\left(1 - \frac{x}{k}\right) - m_1xy,$$
$$\frac{dy}{dt} = e_1m_1xy - m_2yz - d_1y,$$
$$\frac{dz}{dt} = e_2m_2yz - d_2z.$$

It should be noted that in [9,24], the parameters m_i are dependent variables of x and y, respectively, leading to ratio-dependent and Hassle-Varley functional responses [24]. On the other hand, they are treated as fixed constants in this analysis, since they are consumption rates.

Unlike previous models, like the ones presented by [9], and [24], the Allee effect in our model (1) will only affect the rate at which the amount of prey is growing. This rate will surely become less. The influence of the Allee effect increases as the number of prey individuals decreases. Moreover, x will begin to decline until it goes extinct if it drops below n_1. Furthermore, the first term $rx\left(1 - \frac{x}{k}\right)\left(1 - \frac{n_1+n_2}{x+n_2}\right)$ will get closer to the logistics model as x grows. We observe that the model (1) has 10 variables before beginning to analyze the system. The dimensionless variables are selected as follows to nondimensionalize and simplify this model:

$$u = \frac{x}{x_s},\ v = \frac{y}{y_s},\ w = \frac{z}{z_s},\ \tau = tr,$$

where $x_s = \frac{r}{e_1m_1}$, $y_s = \frac{r}{m_1}$, and $z_s = \frac{r}{m_2}$. Then the nondimensional model system takes the form

$$\begin{aligned} \frac{du}{d\tau} &= u(1 - a_1u)\left(1 - \frac{b_1+b_2}{u+b_2}\right) - uv = ug_1(u,v,w), \\ \frac{dv}{d\tau} &= uv - vw - a_2v = vg_2(u,v,w), \\ \frac{dw}{d\tau} &= a_3vw - a_4w = wg_3(u,v,w), \end{aligned} \tag{2}$$

where $a_1 = \frac{r}{e_1m_1k}$, $a_2 = \frac{d_1}{r}$, $a_3 = \frac{e_2m_2}{m_1}$, $a_4 = \frac{d_2}{r}$, $b_1 = \frac{e_1m_1n_1}{r}$, and $b_2 = \frac{e_1m_1n_2}{r}$.

Except for the dimensionless parameters e_1 and e_2, the original system (1) had eight parameters. It decreased the number of parameters in the nondimensional system (2) to six to comply with Buckingham's Pi Theorem, which states that the number of parameters in a dimensionless system should be greater than or equal to the number of parameters in the original system less the number of primary dimensions. Additionally, the nondimensionalized system (2) is easier to understand because it is more condensed. For the sake of simplicity, the nondimensionalized system has been the focus of our investigation. Moreover, since the right-hand side functions g_i in system (2) are continuous and have continuous partial derivatives, it is a Lipschitzian function, and hence system (2) has a unique solution fall in the domain $\mathbb{R}^3_+ = \{(u,v,w) \in \mathbb{R}^3 : u(0) \geq 0, v(0) \geq 0, w(0) \geq 0\}$.

3. Stability and bifurcation analysis

This part calculates the stability requirements for each equilibrium point, identifies all potential equilibrium points, and looks at the likelihood of bifurcation around each equilibrium point. According

to the system (2), it is simple to identify the existence of the following equilibrium points.

1) The trivial equilibrium point $E_0 = (0,0,0)$ always exists.

2) The axial equilibria $E_1 = (b_1, 0,0)$ and $E_2 = \left(\frac{1}{a_1}, 0,0\right)$ always exist.

3) The boundary equilibrium point $E_3 = \left(a_2, \frac{(1-a_1a_2)(a_2-b_1)}{a_2+b_2}, 0\right) = (\breve{u}, \breve{v}, 0)$ exists if and only if the following condition holds:

$$\left.\begin{array}{c} b_1 < a_2 < \frac{1}{a_1} \\ or \\ \frac{1}{a_1} < a_2 < b_1 \end{array}\right\}. \tag{3}$$

Condition (3) guarantees that the numerator of $\breve{v}$ is positive.

4) The positive interior equilibrium point $E_4 = \left(u^*, \frac{a_4}{a_3}, u^* - a_2\right)$, where u^* is the solution to the following equation, which results from the first equation of the system (2):

$$a_1u^2 + \left(\frac{a_4}{a_3} - 1 - a_1b_1\right)u + \frac{a_4b_2}{a_3} + b_1 = 0, \tag{4}$$

that satisfies the following condition:

$$a_2 < u^*. \tag{5}$$

According to Eq (4), there are either two positive roots or zero positive roots when

$$\frac{a_4}{a_3} < 1 + a_1b_1. \tag{6}$$

However, it will be a unique positive interior equilibrium whenever it exists, if, in addition to Conditions (5) and (6), the discriminant of Eq (4) is zero: $\left(\frac{a_4}{a_3} - 1 - a_1b_1\right)^2 = 4a_1\left(\frac{a_4b_2}{a_3} + b_1\right)$.

Now the general Jacobian matrix of the system (2) can be written as

$$D\mathbf{F}(\mathbf{X}) = \begin{pmatrix} g_1 + u\frac{\partial g_1}{\partial u} & -u & 0 \\ v & u - w - a_2 & -v \\ 0 & a_3w & a_3v - a_4 \end{pmatrix}, \tag{7}$$

where

$$g_1 + u\frac{\partial g_1}{\partial u} = -v + (1 - a_1u)\left(1 - \frac{b_1+b_2}{u+b_2}\right) + u\left(\frac{(1-a_1u)(b_1+b_2)}{(u+b_2)^2} - a_1\left(1 - \frac{b_1+b_2}{u+b_2}\right)\right).$$

$\mathbf{F} = (g_1, g_2, g_3)^{\mathrm{T}}$ and $\mathbf{X} = (u, v, w)^{\mathrm{T}}$.

While the second directional derivatives of $\mathbf{F}$ can be computed by

$$D^2\mathbf{F}(\mathbf{X}).(Q.Q) = \begin{pmatrix} q_1\left(\frac{2q_1\left(b_2(b_1+b_2)-a_1(u^3+3u^2b_2+(3u-b_1)b_2^2)\right)}{(u+b_2)^3} - 2q_2\right) \\ 2q_2(q_1-q_3) \\ 2a_3q_2q_3 \end{pmatrix}, \tag{8}$$

where $Q = (q_1, q_2, q_3)^T$ vsn be any nonzero vector.

Consequently, the dynamic behavior around the obtained equilibria is established in the following theorems.

Theorem 1. *The trivial equilibrium point of the system (2) is unconditionally locally asymptotic stable. It will be globally asymptotically stable, provided that*

$$b_1 = \frac{1}{a_1}. \tag{9}$$

Proof. The Jacobian matrix (7) at the trivial equilibrium point becomes

$$J(E_0) = \begin{pmatrix} -\frac{b_1}{b_2} & 0 & 0 \\ 0 & -a_2 & 0 \\ 0 & 0 & -a_4 \end{pmatrix}.$$

Thus, there are three negative eigenvalues $\left(-\frac{b_1}{b_2}, -a_2, -a_4\right)$, which lead to a solution that is unconditionally locally asymptotically stable at the point E_0.

To investigate under which conditions E_0 would be globally asymptotically stable, consider the following function $L_1 = u + v + \frac{w}{a_3}$, which is a real-valued positive definite function at E_0. Now the derivative of L_1 can be written as

$$\frac{dL_1}{d\tau} = u(1-a_1u)\left(\frac{u-b_1}{u+b_2}\right) - a_2v - \frac{a_4}{a_3}w = a_1u\left(\frac{1}{a_1}-u\right)\left(\frac{u-b_1}{u+b_2}\right) - a_2v - \frac{a_4}{a_3}w.$$

Consequently, under condition (9), the term $a_1u\left(\frac{1}{a_1}-u\right)\left(\frac{u-b_1}{u+b_2}\right) = a_1u(b_1-u)\left(\frac{u-b_1}{u+b_2}\right) < 0$ for all values of $0 < u < b_1$ or $u > b_1$. Hence $\frac{dL_1}{d\tau}$ is a negative definite that makes E_0 globally asymptotically stable.

However, for $u = b_1$, the derivative $\frac{dL_1}{d\tau} = -a_2v - \frac{a_4}{a_3}w$ becomes a negative semidefinite that makes E_0 a stable point. So, by using Lasalle's invariance principle [11], and the fact that the point E_0 is the only invariant set within the set of points, this makes $\frac{dL_1}{d\tau} = 0$. Hence, the trivial point is also attractive. Hence, it is asymptotical stable. Moreover, since the function L_1 is readily unbounded, E_0 is globally asymptotically stable. Thus, the proof is done.

Since the trivial equilibrium is a structurally stable point and is unconditionally asymptotically stable, bifurcation cannot occur close to it, as demonstrated by the aforementioned theorem. Furthermore, it is globally asymptotically stable under condition (9), which means the two axial points E_1 and E_2 coincide with each other, and the carrying capacity (k) is equal to the critical value of the Allee effect (n_1).

Theorem 2. *When $b_1 \neq \frac{1}{a_1}$, the axial points E_1 and E_2 satisfy the following:*

1) The point E_1 is locally asymptotically stable if and only if $\frac{1}{a_1} < b_1 < a_2$.

2) The point E_1 *is a saddle point for* $b_1 < \frac{1}{a_1}$ *or* $a_2 < b_1$.

3) If a_2 *passes through the value* $a_2{}^* = b_1$*, then a transcritical bifurcation takes place around the point* E_1.

4) The point E_2 *is locally asymptotically stable if and only if* $b_1 < \frac{1}{a_1} < a_2$.

5) The point E_2 *is a saddle point for* $\frac{1}{a_1} < b_1$ *or* $a_2 < \frac{1}{a_1}$.

6) *If* a_2 *passes through the value* $a_2{}^* = \frac{1}{a_1}$*, then a transcritical bifurcation takes place around the point* E_2.

Proof. Direct computation shows that the Jacobian matrix (7) at the axial points E_1 and E_2, respectively, becomes

$$J(E_1) = \begin{pmatrix} \frac{b_1 a_1\left(\frac{1}{a_1} - b_1\right)}{b_1 + b_2} & -b_1 & 0 \\ 0 & -a_2 + b_1 & 0 \\ 0 & 0 & -a_4 \end{pmatrix}, \text{ and } J(E_2) = \begin{pmatrix} \frac{b_1 - \frac{1}{a_1}}{\frac{1}{a_1} + b_2} & -\frac{1}{a_1} & 0 \\ 0 & \frac{1}{a_1} - a_2 & 0 \\ 0 & 0 & -a_4 \end{pmatrix}.$$

The eigenvalues of $J(E_1)$ are determined by $\lambda_{11} = \frac{b_1 a_1\left(\frac{1}{a_1} - b_1\right)}{b_1 + b_2}$, $\lambda_{12} = -a_2 + b_1$, and $\lambda_{13} = -a_4$, which are negative under the condition given in Part (1). However, $\lambda_{11} > 0$ or $\lambda_{12} > 0$ under the conditions given in Part (2). Hence, the proofs of Parts (1) and (2) are done.

Now, to prove Part (3), when $a_2 = a_2{}^* = b_1$, the Jacobian matrix $J(E_1)$ becomes

$$J_1 = J(E_1, a_2{}^*) = \begin{pmatrix} \frac{b_1 a_1\left(\frac{1}{a_1} - b_1\right)}{b_1 + b_2} & -b_1 & 0 \\ 0 & 0 & 0 \\ 0 & 0 & -a_4 \end{pmatrix}.$$

Thus the eigenvalues become $\lambda_{11} = \frac{b_1 a_1\left(\frac{1}{a_1} - b_1\right)}{b_1 + b_2}$, $\lambda_{12} = 0$, and $\lambda_{13} = -a_4$, which makes E_1 a nonhyperbolic point. Let $Q_1 = (q_{11}, q_{12}, q_{13})^T$ and $P_1 = (p_{11}, p_{12}, p_{13})^T$ are the eigenvectors of J_1 and ${J_1}^T$ corresponding to $\lambda_{12} = 0$. Direct computation gives the following:

$$Q_1 = \left(\frac{b_1 + b_2}{(1 - a_1 b_1)}, 1, 0\right)^T, \text{ and } P_1 = (0,1,0)^T.$$

Moreover, it can be obtained that

$$\frac{\partial \mathbf{F}}{\partial a_2} = \mathbf{F}_{a_2} = (0, -v, 0)^{\mathrm{T}} \Rightarrow \mathbf{F}_{a_2}(E_1, a_2{}^*) = (0,0,0)^{\mathrm{T}}.$$

Thus ${P_1}^T \mathbf{F}_{a_2}(E_1, a_2{}^*) = 0$. Hence, a saddle node cannot occur. In addition

$$D\mathbf{F}_{a_2} = \begin{pmatrix} 0 & 0 & 0 \\ 0 & -1 & 0 \\ 0 & 0 & 0 \end{pmatrix} \Rightarrow D\mathbf{F}_{a_2}(E_1, a_2{}^*).Q_1 = \begin{pmatrix} 0 \\ -1 \\ 0 \end{pmatrix}.$$

Thus

$$P_1{}^T\left[D\mathbf{F}_{a_2}(E_1, a_2{}^*).Q_1\right] = -1.$$

Now according to Eq (8), the second derivative becomes

$$D^2\mathbf{F}(E_1, a_2{}^*).(Q_1.Q_1) = \begin{pmatrix} \frac{b_1+b_2}{(1-a_1b_1)}\left(\frac{2q_1\left[b_2(b_1+b_2)-a_1b_1(b_1{}^2+3b_1b_2+2b_2^2)\right]}{(b_1+b_2)^3} - 2\right) \\ 2\frac{b_1+b_2}{(1-a_1b_1)} \\ 0 \end{pmatrix}.$$

Therefore, it can be obtained that

$$P_1{}^T[D^2\mathbf{F}(E_1, a_2{}^*).(Q_1.Q_1)] = 2\frac{b_1+b_2}{(1-a_1b_1)} \neq 0.$$

Hence, according to the Sotomayor theorem [26], a transcritical bifurcation occurs around E_1.

Now, to prove Parts (4) and (5), the eigenvalues of $J(E_2)$ are determined by $\lambda_{21} = \frac{b_1-\frac{1}{a_1}}{\frac{1}{a_1}+b_2}$, $\lambda_{22} = \frac{1}{a_1} - a_2$, and $\lambda_{23} = -a_4$, which are negative under the condition given in Part (4). However, $\lambda_{21} > 0$ or $\lambda_{22} > 0$ under the conditions given in Part (5). Hence the proofs of Parts (4) and (5) are done.

To prove Part (6), when $a_2 = a_2{}^* = \frac{1}{a_1}$, the Jacobian matrix $J(E_2)$ becomes

$$J_2 = J(E_2, a_2{}^*) = \begin{pmatrix} \frac{b_1-\frac{1}{a_1}}{\frac{1}{a_1}+b_2} & -\frac{1}{a_1} & 0 \\ 0 & 0 & 0 \\ 0 & 0 & -a_4 \end{pmatrix}.$$

Thus the eigenvalues become $\lambda_{21} = \frac{b_1-\frac{1}{a_1}}{\frac{1}{a_1}+b_2}$, $\lambda_{22} = 0$, and $\lambda_{23} = -a_4$, which makes E_2 a nonhyperbolic point. Let $Q_2 = (q_{21}, q_{22}, q_{23})^T$ and $P_2 = (p_{21}, p_{22}, p_{23})^T$ are the eigenvectors of J_2 and $J_2{}^T$ corresponding to $\lambda_{22} = 0$. Direct computation shows that

$$Q_2 = \left(\frac{\frac{1}{a_1}+b_2}{a_1\left(b_1-\frac{1}{a_1}\right)}, 1, 0\right)^T, \text{ and } P_2 = (0,1,0)^T.$$

Moreover, it can be obtained that

$$\mathbf{F}_{a_2} = (0, -v, 0)^{\mathrm{T}} \Rightarrow \mathbf{F}_{a_2}(E_2, a_2{}^*) = (0,0,0)^{\mathrm{T}}.$$

Thus $P_2{}^T\mathbf{F}_{a_2}(E_2, a_2{}^*) = 0$. Hence a saddle node cannot occur. In addition

$$D\mathbf{F}_{a_2} = \begin{pmatrix} 0 & 0 & 0 \\ 0 & -1 & 0 \\ 0 & 0 & 0 \end{pmatrix} \Rightarrow D\mathbf{F}_{a_2}(E_2, a_2{}^*).Q_2 = \begin{pmatrix} 0 \\ -1 \\ 0 \end{pmatrix}.$$

Thus

$$P_2{}^T\left[D\mathbf{F}_{a_2}(E_1, a_2{}^*).Q_2\right] = -1.$$

Now according to Eq (8), the second derivative becomes

$$D^2\mathbf{F}(E_2, a_2{}^*).(Q_2.Q_2) = \begin{pmatrix} \left(\frac{1+a_1b_2}{a_1(a_1b_1-1)}\right)\left(\frac{2\left(\frac{1+a_1b_2}{a_1(a_1b_1-1)}\right)\left(b_2(b_1+b_2)-a_1\left(\left(\frac{1}{a_1}\right)^3+3\left(\frac{1}{a_1}\right)^2b_2+\left(3\left(\frac{1}{a_1}\right)-b_1\right)b_2^2\right)\right)}{\left(\left(\frac{1}{a_1}\right)+b_2\right)^3}-2\right) \\ 2\left(\frac{1+a_1b_2}{a_1(a_1b_1-1)}\right) \\ 0 \end{pmatrix}.$$

Therefore, it is found that

$$P_2{}^T[D^2\mathbf{F}(E_2, a_2{}^*).(Q_2.Q_2)] = 2\left(\frac{1+a_1b_2}{a_1(a_1b_1-1)}\right) \neq 0.$$

Hence, according to the Sotomayor theorem, a transcritical bifurcation takes place around E_2. Thus, the proof is complete.

Note that since all the eigenvalues of $J(E_1)$ and $J(E_2)$ are real, a Hopf bifurcation does not exist.

On the other hand, when $b_1 = \frac{1}{a_1}$, the two axial equilibrium points E_1 and E_2 coincide with each other and become, say, $E = (b_1, 0,0)$, and the Jacobian matrix around this point is written

$$J(E) = \begin{pmatrix} 0 & -b_1 & 0 \\ 0 & -a_2 + b_1 & 0 \\ 0 & 0 & -a_4 \end{pmatrix}.$$

Hence the eigenvalues are $(0,-a_2 + b_1,-a_4)$, which means that E is a nonhyperbolic point, and their stability cannot be studied using the linearization technique. Moreover, the boundary equilibrium point E_3 will not exist, as condition (3) is not satisfied.

Theorem 3. *The boundary equilibrium point E_3 is locally asymptotically stable if the following conditions hold:*

$$\frac{(1-a_1a_2)a_3(a_2-b_1)}{a_2+b_2} < a_4, \tag{10}$$

$$\frac{(b_1+b_2)}{a_2{}^2+2a_2b_2-b_1b_2} < a_1. \tag{11}$$

If we reverse one of the two conditions (10) or (11), then it is a saddle point. Moreover, if condition (11) holds with $a_4 = \frac{(1-a_1a_2)a_3(a_2-b_1)}{a_2+b_2}$ $(\equiv a_4{}^*)$, then the system (2) undergoes a transcritical bifurcation. However, when condition (10) holds with $a_1 = \frac{(b_1+b_2)}{a_2(b_1+b_2)+(a_2-b_1)(a_2+b_2)}$ $(\equiv a_1{}^*)$, then the system (2) undergoes a Hopf bifurcation, provided that

$$a_2(b_1 + b_2) + (a_2 - b_1)(a_2 + b_2) > 0. \tag{12}$$

Proof. The Jacobian matrix (7) at the point E_3 becomes

$$J(E_3)=\begin{pmatrix} a_2\frac{(1-a_1a_2)(b_1+b_2)-a_1(a_2-b_1)(a_2+b_2)}{(a_2+b_2)^2} & -a_2 & 0 \\ \frac{(1-a_1a_2)(a_2-b_1)}{a_2+b_2} & 0 & -\frac{(1-a_1a_2)(a_2-b_1)}{a_2+b_2} \\ 0 & 0 & -a_4+\frac{(1-a_1a_2)a_3(a_2-b_1)}{a_2+b_2} \end{pmatrix}=(c_{ij}).$$

Thus the characteristic polynomial of $J(E_3)$ can be written as

$$[\lambda^2-c_{11}\lambda-c_{12}c_{21}](\lambda-c_{33})=0.$$

Therefore, the eigenvalues are written as $\lambda_{31},\lambda_{32}=\frac{c_{11}}{2}\pm\frac{\sqrt{{c_{11}}^2+4c_{12}c_{21}}}{2}$, and $\lambda_{33}=c_{33}$. It is easy to verify that conditions (10) and (11) lead to $c_{33}<0$ and $c_{11}<0$, respectively. Thus, using the existence condition (3), the eigenvalues λ_{31} and λ_{32} are negative or have negative real parts, while the third eigenvalue λ_{33} is negative under the given conditions. Therefore, E_3 is locally asymptotically stable.

Now, reversing condition (10) yields $\lambda_{33}>0$, while reversing condition (11) means that λ_{31} and λ_{32} have positive real parts, and hence E_3 becomes the saddle point.

For $a_4=a_4{}^*$, the element $c_{33}=0$; therefore, $J_3=J(E_3,a_4{}^*)$ has a zero eigenvalue with two negative real parts due to condition (11). So E_3 becomes a nonhyperbolic point.

Let $Q_3=(q_{31},q_{32},q_{33})^T$ and $P_3=(p_{31},p_{32},p_{33})^T$ be the eigenvectors of J_3 and ${J_3}^T$ corresponding to $\lambda_{33}=0$. Direct computation gives

$$Q_3=\left(1,-\frac{c_{11}}{c_{12}},1\right)^T \text{ and } P_3=(0,0,1)^T.$$

Moreover, it is found that

$$\mathbf{F}_{a_4}=(0,0,-w)^{\mathrm{T}} \Rrightarrow \mathbf{F}_{a_4}(E_3,a_4{}^*)=(0,0,0)^{\mathrm{T}}.$$

Thus ${P_3}^T\mathbf{F}_{a_4}(E_3,a_4{}^*)=0$. Hence, a saddle node cannot occur. In addition

$$D\mathbf{F}_{a_4}=\begin{pmatrix}0&0&0\\0&0&0\\0&0&-1\end{pmatrix} \Rrightarrow D\mathbf{F}_{a_4}(E_3,a_4{}^*).Q_3=\begin{pmatrix}0\\0\\-1\end{pmatrix}.$$

Thus

$$P_3{}^T\left[D\mathbf{F}_{a_4}(E_3,a_4{}^*).Q_3\right]=-1.$$

Now, according to Eq (8), the second derivative becomes

$$D^2\mathbf{F}(E_3,a_4{}^*).(Q_3.Q_3)=\begin{pmatrix}\left(\frac{2\left(b_2(b_1+b_2)-a_1({a_2}^3+3{a_2}^2b_2+(3a_2-b_1)b_2^2)\right)}{(a_2+b_2)^3}+2\frac{c_{11}}{c_{12}}\right)\\0\\-2a_3\frac{c_{11}}{c_{12}}\end{pmatrix}.$$

Therefore, it is found that

$$P_3{}^T[D^2\mathbf{F}(E_3, a_4{}^*).(Q_3.Q_3)] = -2a_3\frac{c_{11}}{c_{12}} \neq 0.$$

Hence, according to the Sotomayor theorem, a transcritical bifurcation occurs around E_3.

Finally, for $a_1 = a_1{}^*$, the element $c_{11} = 0$; therefore, $J_{33} = J(E_3, a_1{}^*)$ has two pure imaginary eigenvalues $\lambda_{31}, \lambda_{32} = \pm i\sqrt{a_2\frac{(1-a_1{}^*a_2)(a_2-b_1)}{a_2+b_2}}$, and $\lambda_{33} = c_{33} < 0$ due to condition (10). Accordingly, in the neighborhood of $a_1{}^*$, the eigenvalues λ_{31} and λ_{32} becomes complex; say, $\lambda_{31}, \lambda_{32} = \alpha \pm i\beta$, with $\alpha(a_1) = \frac{c_{11}}{2}$, $\alpha(a_1{}^*) = 0$, and $\beta(a_1) > 0$. Consequently, the system undergoes a Hopf bifurcation if the following transversality condition holds: $\frac{d\alpha(a_1)}{da_1}\Big|_{a_1=a_1{}^*} \neq 0$. Direct computation with the help of condition (12) gives

$$\frac{1}{2}\frac{dc_{11}}{da_1}\Big|_{a_1=a_1{}^*} = \frac{1}{2}\left(a_2\frac{-a_2(b_1+b_2)-(a_2-b_1)(a_2+b_2)}{(a_2+b_2)^2}\right) < 0.$$

Hence, Hopf bifurcation takes place, and thus the proof is complete.

Theorem 4. *The positive interior equilibrium point* $E_4 = (u^*, v^*, w^*) = \left(u^*, \frac{a_4}{a_3}, u^* - a_2\right)$ *is locally asymptotically stable if the following condition holds:*

$$(b_1 + b_2) + a_1b_1b_2 < a_1(u^{*2} + 2b_2u^*). \tag{13}$$

Proof. The Jacobian matrix (7) at the point E_4 becomes

$$J(E_4) = \begin{pmatrix} \rho_{11} & -u^* & 0 \\ \frac{a_4}{a_3} & 0 & -\frac{a_4}{a_3} \\ 0 & a_3(u^* - a_2) & 0 \end{pmatrix},$$

where $\rho_{11} = u^*\left(\frac{(b_1+b_2)-a_1(u^{*2}+2b_2u^*-b_1b_2)}{(u+b_2)^2}\right)$. The characteristic polynomial equation of $J(E_4)$ is determined by

$$\lambda^3 + A_1\lambda^2 + A_2\lambda + A_3 = 0, \tag{14}$$

where

$$A_1 = -\rho_{11},$$

$$A_2 = \left(\frac{a_4}{a_3}\right)[u^* + a_3(u^* - a_2)],$$

$$A_3 = -\left(\frac{a_4}{a_3}\right)a_3(u^* - a_2)\rho_{11},$$

with

$$A_1A_2 - A_3 = -\left(\frac{a_4}{a_3}\right)u^*\rho_{11}.$$

Consequently, all the requirements of the Routh-Hurwitz criterion, which are given by $A_1 > 0$, $A_3 > 0$, and $A_1A_2 - A_3 > 0$, to have negative real parts in the eigenvalues (roots) of Eq (14) are

satisfied if and only if condition (13) holds. Therefore, E_4 is locally asymptotically stable.

Note that since the positive interior equilibrium, whenever it exists, will not be unique, and the trivial equilibrium point always exists and is unconditionally asymptotically stable, then the positive point E_4 cannot be globally stable. However, when the inequality changes to equality in condition (12), the value of ρ_{11} becomes zero. Hence, Eq (14) becomes $\lambda^3 + A_2\lambda = 0$, which gives three roots $\lambda_{41,42} = \pm i\sqrt{A_2}$, and $\lambda_{43} = 0$. Therefore, Hopf bifurcation around the positive interior equilibrium point cannot occur because the real part always has a zero value.

4. Numerical simulation

To make our research more practical, numerical methods are utilized to simulate the behaviors of the equilibria that have been analyzed. The objectives were to confirm our obtained findings and specify the role of each parameter in the dynamic system's behavior. To reach these objectives, a hypothetical set of parameter values are given below that are biologically feasible for a wide range of food chain systems is used throughout this section.

$$a_1 = 0.1, a_2 = 0.1, a_3 = 0.25, a_4 = 0.15, b_1 = 0.2, b_2 = 0.2. \tag{15}$$

By solving system (2) using dde45 Matlab code and the dataset of (15), starting from various initial points, we observed that the solutions of system (2) asymptotically approached $E_0 = (0,0,0)$ and $E_4 = (3.19,0.59,3.1)$ simultaneously, which means that bistable behavior occurs between these two equilibrium points (see Figure 1). Note that in the following figures, the red dot and blue dot stand for the attracting equilibrium points and initial points, respectively.

From Figure 1, it is concluded that there is no global stability regarding the positive equilibrium point; instead, the positive point is locally asymptotically stable, as condition (13) holds using the dataset of (15). Hence, each of the points E_0 and E_4 has its specific basin of attraction that gives the system its bistable behavior.

The aforementioned findings might be understood as follows. There may be two basins of attraction in the food chain model, one of which leads to the trivial equilibrium and the other to the positive equilibrium. Which equilibrium the system converges to is determined by initial population densities or outside influences. From a biological perspective, this implies that the ecosystem is susceptible to both the original conditions and outside influences. The balance between survival and collapse could be tipped by minor adjustments.

Now the role of varying the system's parameters is investigated. It was found that when we vary the parameter a_1 in the ranges of $a_1 < 0.15$ and $a_1 \geq 0.15$, the system (2) has bistable behavior between E_0 with E_4, and was globally asymptotically stable at E_0; see Figure 1 for the first range and Figure 2 for the second range.

Figure 2 shows the global stability of E_0 in the range $a_1 \geq 0.15$ as the axial points are saddle points, while the boundary equilibrium point E_3 and the positive equilibrium point (E_4) do not exist because the roots of Eq (4) are complex numbers. A bifurcation diagram as a function of a_1 in the range $0 \leq a_1 \leq 0.25$ is also added to confirm the transmission of the dynamics from E_4 to E_0 at the bifurcation value $a_1 = 0.15$; see Figure 3. Further numerical analysis shows that varying the parameters a_4, b_1, and b_2 has a similar influence on the dynamic behavior of the system (2) to that shown for a_1.

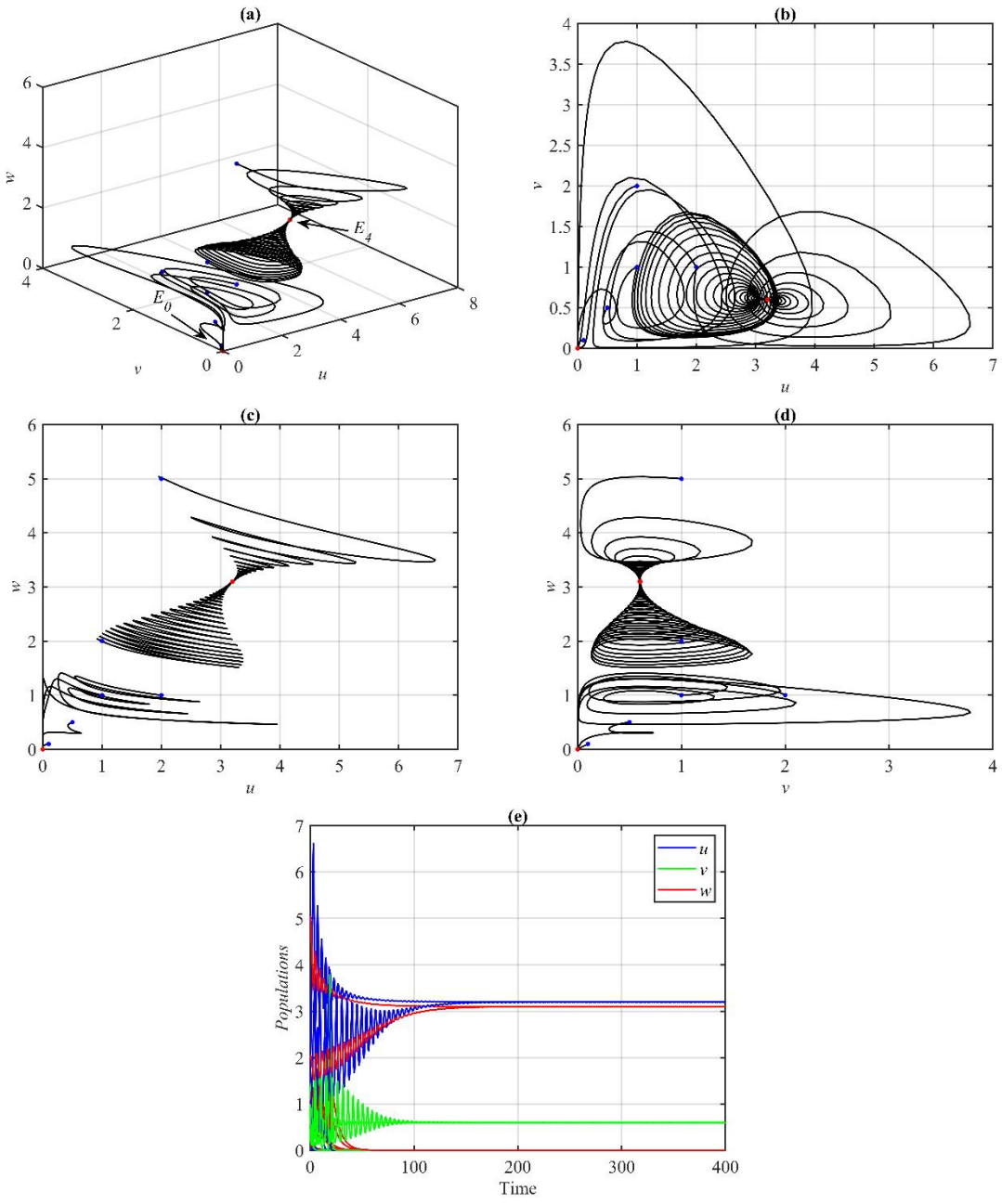

Figure 1. The solutions of system (2) using the dataset (15) and starting from different initial points approach E_0 and E_4 simultaneously, indicating bistable behavior. (a) Bistable dynamics in a three-dimensional (3D) phase portrait. (b) The projection in the uv-plane. (c) The projection in the uw-plane. (d) The projection in the vw-plane. (e) The time series.

One or more populations in the food chain achieve zero density, which is known as a trivial equilibrium point. According to biology, this means that a predator population may become extinct if its prey becomes too scarce, or a prey population may plummet as a result of overpredation or a lack of resources. When at least one species is unable to endure under the current dynamics, this usually signifies an unstable or unsustainable condition of the ecosystem.

Now, varying the parameter a_2 in the range of $a_2 < 3.38$ and $a_2 \geq 3.38$ makes the system (2) undergo bistability between E_0 and E_4 for the first range and bistability between E_0 and E_3 for the second range; see Figures 4 and 5 for selected values.

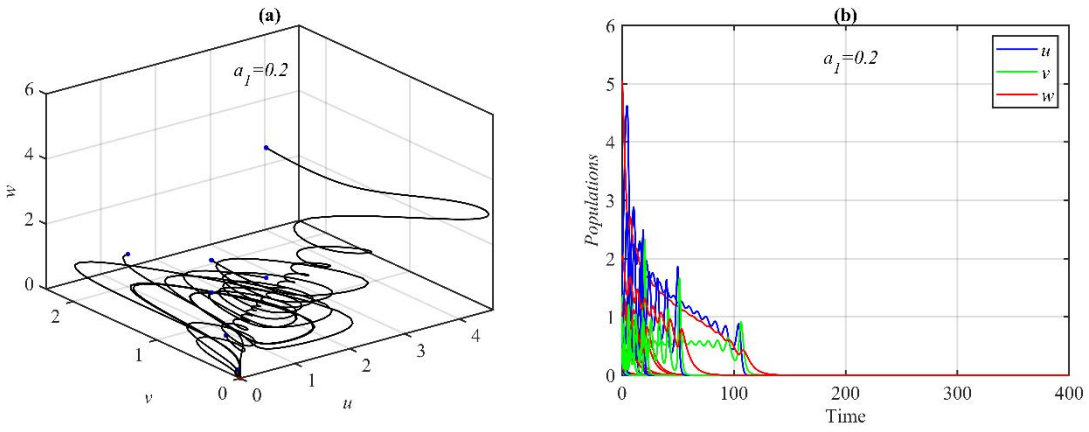

Figure 2. The solutions of the system (2) using the dataset (15) and starting from different initial points with $a_1 = 0.2$ asymptotically approach (a) E_0 in a 3D phase portrait. (b) The time series.

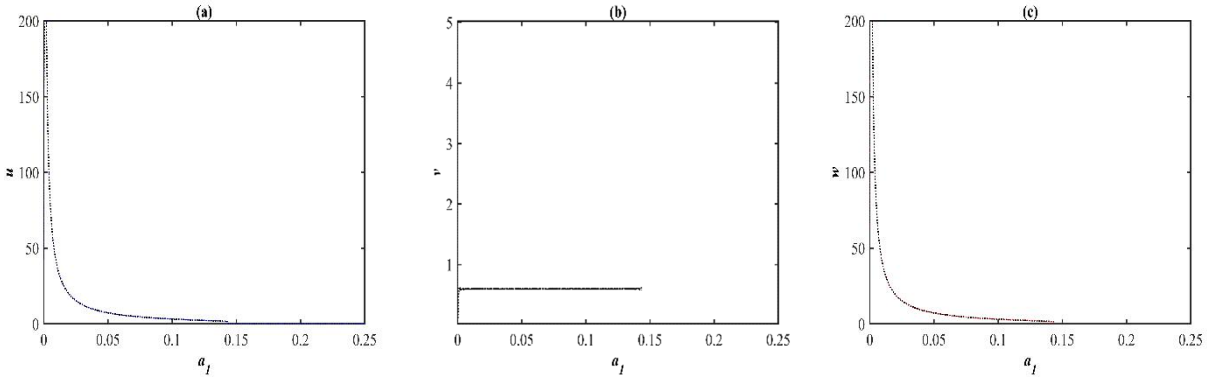

Figure 3. The bifurcation diagrams of the system (2) using the dataset (15) with $0 \leq a_1 \leq 0.25$ and starting from the initial point (2,1,5). (a) The trajectory of u as a function of a_1. (b) The trajectory of v as a function of a_1. (c) The trajectory of w as a function of a_1.

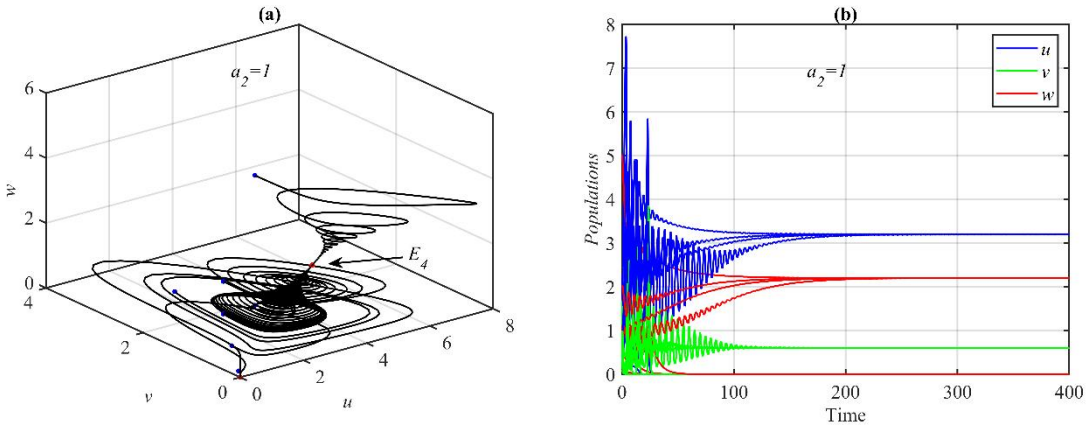

Figure 4. The solutions of the system (2) using the dataset (15) and starting from different initial points with $a_2 = 1$ asymptotically approach E_0 and $E_4 = (3.19,0.6,2.2)$ simultaneously. (a) Bistability in a 3D phase portrait. (b) The time series.

Figure 5 shows the transfer from bistable behavior between E_0 and E_4 to bistable behavior between E_0 and E_3 when the positive equilibrium point disappears, while the boundary equilibrium point exists and their stability conditions are satisfied. Moreover, a bifurcation diagram, as a function of a_2 in the range $0.1 \leq a_4 \leq 4$, is added to confirm the transmission of the dynamics from E_4 to E_3 at the bifurcation value $a_2 = 3.38$; see Figure 6.

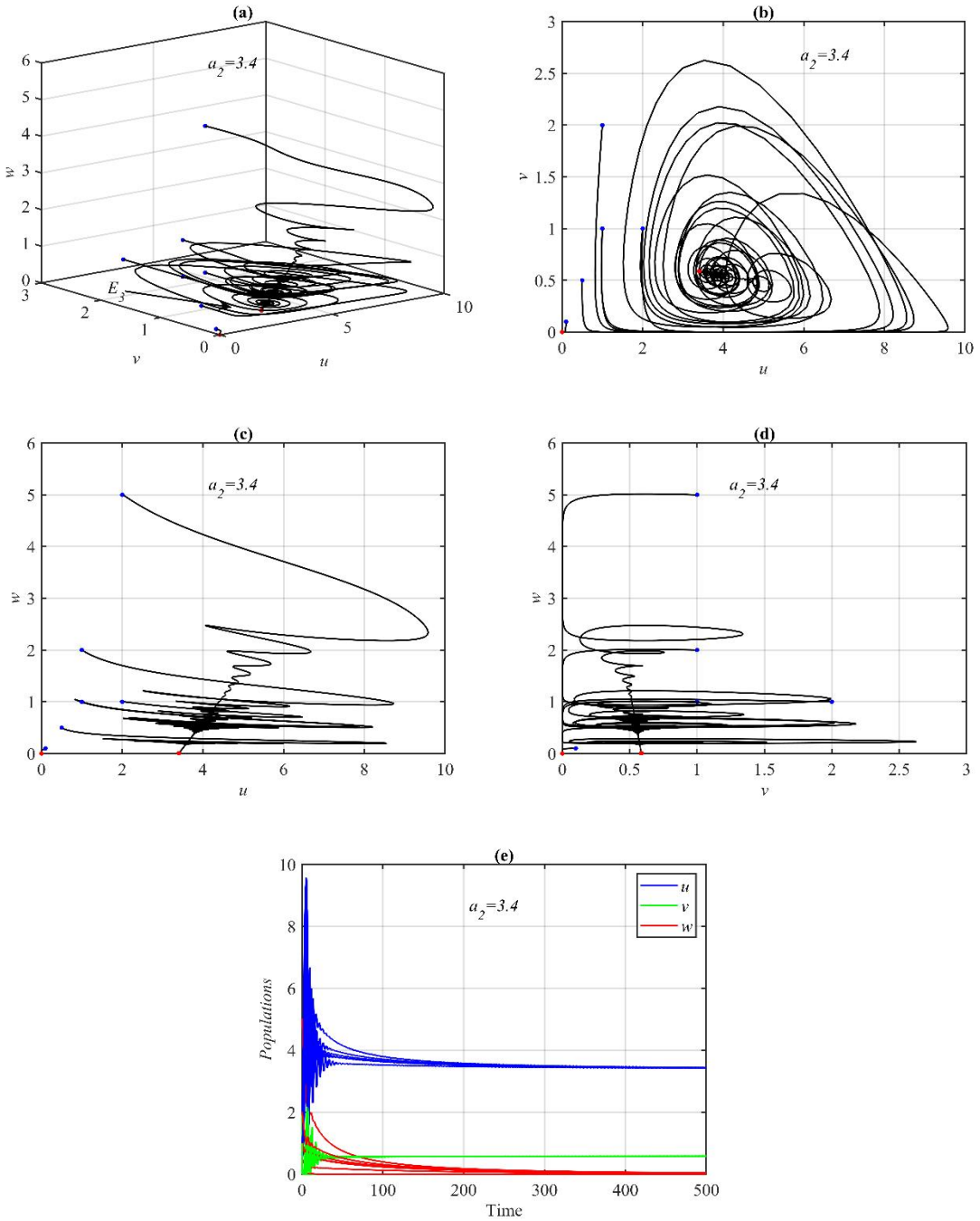

Figure 5. The solutions of the system (2) using the dataset (15) and starting from different initial points with $a_2 = 3.4$ approach E_0 and $E_3 = (3.4,0.58,0)$ simultaneously, indicating bistable behavior. (a) Bistable dynamics in a 3D phase portrait. (b) The projection in the uv-plane. (c) The projection in the uw-plane. (d) The projection in the vw-plane. (e) The time series.

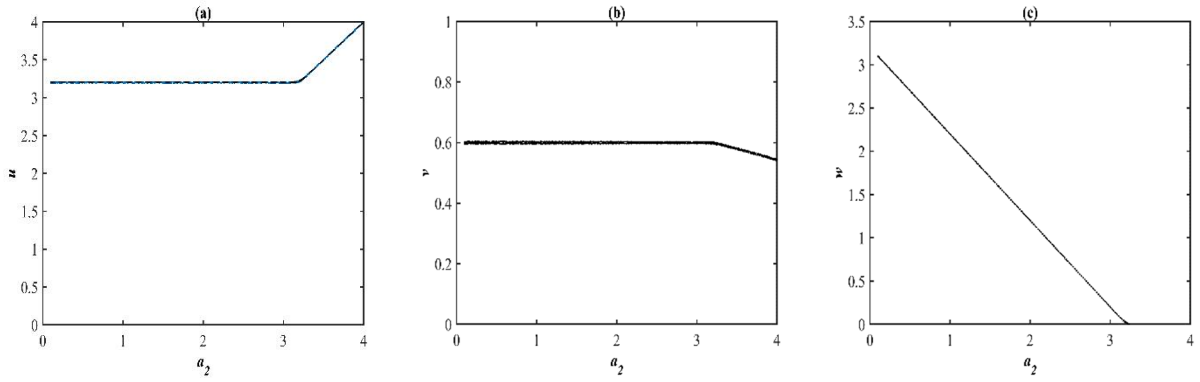

Figure 6. The bifurcation diagrams of the system (2) using the dataset (15) with $0.1 \leq a_2 \leq 4$, and starting from the initial point (2,1,5). (a) The trajectory of u as a function of a_2. (b) The trajectory of v as a function of a_2. (c) The trajectory of w as a function of a_2.

Moreover, it is observed that the system (2) asymptotically approaches E_0 and is bistable between E_0 and E_4 when the parameter a_3 belongs to the ranges $a_3 < 0.23$ and $a_3 \geq 0.23$, respectively, as explained in Figures 7 and 8.

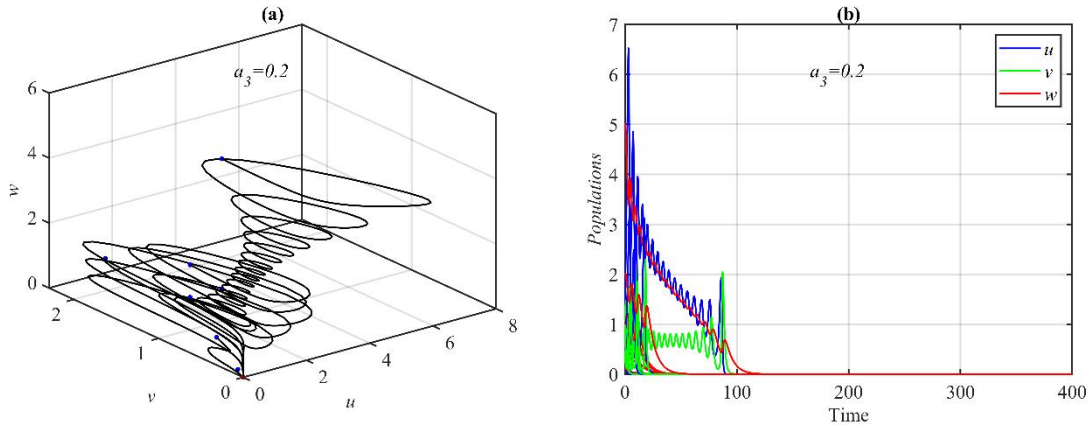

Figure 7. The solutions of the system (2) using the dataset (15) and starting from different initial points with $a_3 = 0.2$ asymptotically approach (a) E_0 in a 3D phase portrait. (b) The time series.

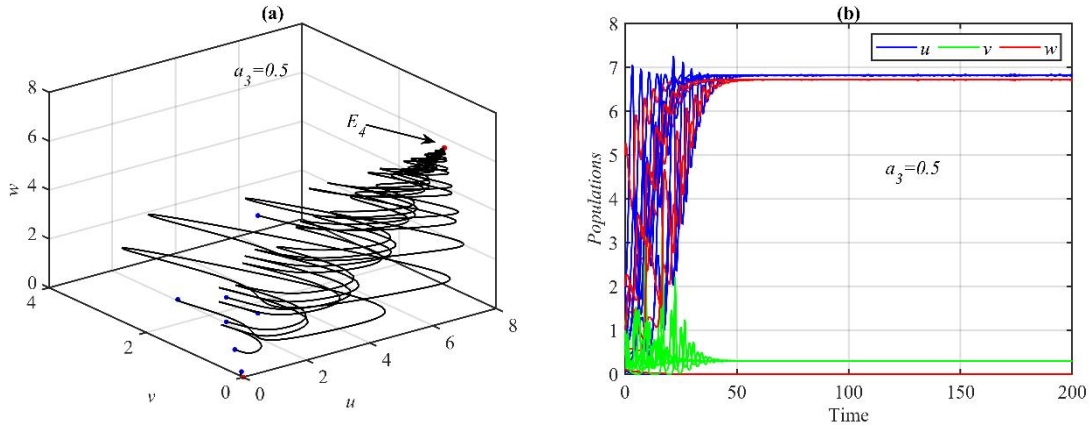

Figure 8. The solutions of the system (2) using the dataset (15) and starting from different initial points with $a_3 = 0.5$ asymptotically approach E_0 with $E_4 = (6.81,0.29,6.71)$ simultaneously. (a) Bistability in a 3D phase portrait. (b) The time series.

Finally, to confirm the results of Theorem 2, the system (2) is solved using the dataset (15) with $a_1 = 15$ and $b_1 = 0.08$. Where the conditions in the first and fifth points of Theorem 2 are satisfied for this set of parameter values, it is found that the system (2) has bistable behavior between E_0 and $E_1 = (b_1, 0,0)$, as shown in Figure 9.

Direct computation shows that both the axial points E_1 and E_2 exist, but E_1 is asymptotically stable while E_2 is a saddle point.

On the other hand, the system (2) is solved using the dataset (15) with $a_1 = 15$ and $b_1 = 0.05$. Where the conditions in the second and fourth points of Theorem 2 are satisfied for this set of parameter values, it is found that the system (2) has bistable behavior between E_0 and $E_2 = (\frac{1}{a_1}, 0,0)$ as shown in Figure 10.

Direct computation shows that both the axial points E_1 and E_2 exist, but E_2 is asymptotically stable while E_1 is a saddle point.

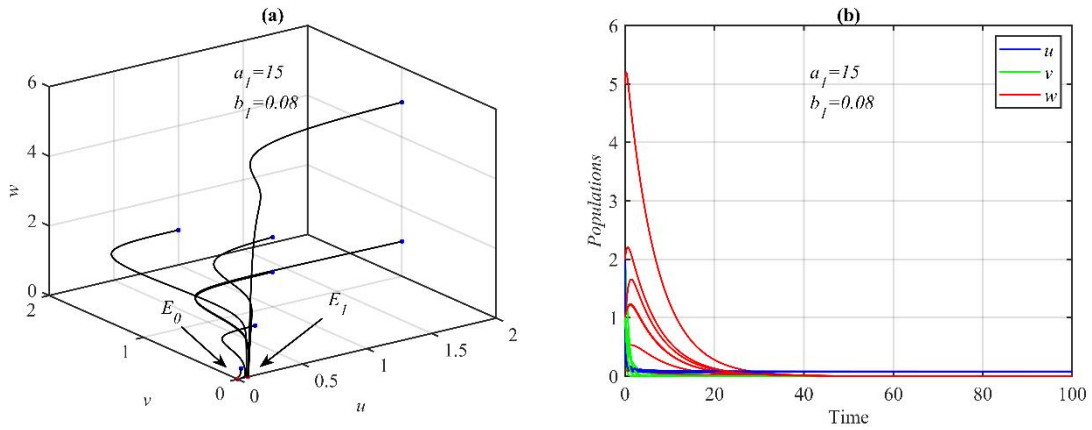

Figure 9. The solutions of the system (2) using the dataset (15) and starting from different initial points with $a_1 = 15$ and $b_1 = 0.08$ asymptotically approach E_0 and $E_1 = (0.08,0,0)$ simultaneously. (a) Bistability in a 3D phase portrait. (b) The time series.

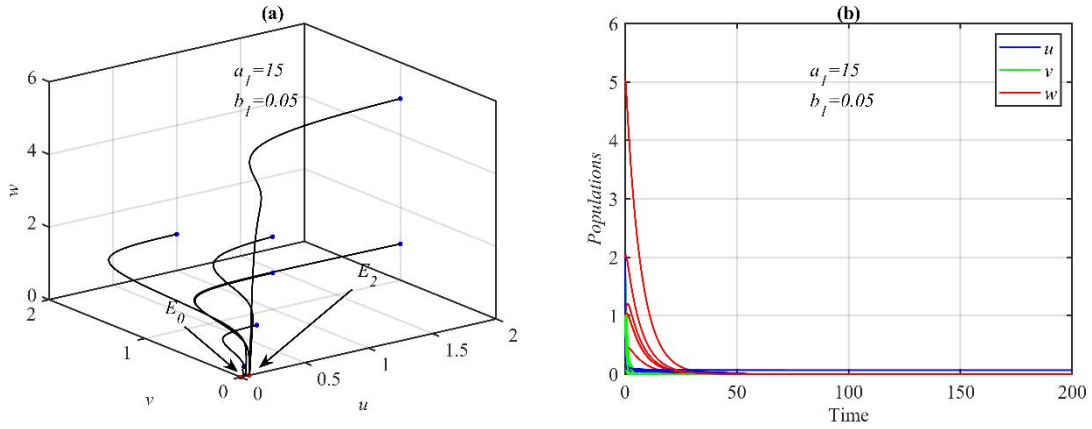

Figure 10. The solutions of the system (2) using the dataset (15) and starting from different initial points with $a_1 = 15$ and $b_1 = 0.05$ asymptotically approach E_0 and $E_2 = (0.06,0,0)$ simultaneously. (a) Bistability in a 3D phase portrait. (b) The time series.

5. Discussion

To describe the analytical results, the stability analysis is discussed first. Regarding stability, Theorem 2 establishes that E_0 is globally asymptotically stable when $b_1 = \frac{1}{a_1}$ and that the other points are unstable in this scenario wherever they are present. In addition, it is demonstrated that global stability can only be attained at the trivial equilibrium point by examining the behavior of this crucial consequence. This is because the system (2) always converges to E_0 under the starting condition $u_0 < \min\left\{\frac{1}{a_1}, b_1\right\}$, which is clear from the first equation of the system (2). This indicates that regardless of the initial condition, there is no scenario in which the system would converge to one of the other equilibrium points. As a result, the other equilibrium points are always either unstable or locally asymptotically stable.

Next, regarding the bifurcation, Hopf bifurcations for the boundary equilibrium point and the positive interior equilibrium point are discussed, as there is a possibility of having complex eigenvalues in these two cases only. However, it is proven that Hopf bifurcation may occur around the boundary point, while it does not exist around the positive point. On the other hand, Theorems 2 and 3 revealed the possibility of having a transcritical bifurcation near the axial points and boundary points under certain conditions.

6. Conclusions

In this paper, the behaviors of the equilibria of the food chain model with the Allee effect, in general, are investigated. Analytically, the equilibrium points have been computed and further classified. Additionally, the stability and bifurcation analyses have been completed. Numerically, realistic data are used to analyze the equilibrium points. All the numerical results match the analytical results. This verifies the results obtained by the analytical methods. Moreover, the model's features have been visually displayed by conducting numerical simulations. It is summarized below. The system does not have global stability except at the trivial equilibrium point; instead, the system has bistable cases due to a specific basin of attraction for each point. Decreasing the carrying capacity, increasing the

superpredator death rate, or increasing the Allee effect rate lead to the system's collapse, and the system approaches a trivial point globally. The increase in predator death rates leads to the extinction of the superpredator. Finally, the increase in the conversion rate of biomass to the superpredator keeps the possibility of persisting at a positive equilibrium point under certain conditions and initial points.

The data above suggest that the model may contain crucial thresholds (e.g., the lowest amount of prey required for maintaining predators). The system transitions from coexistence to extinction if these thresholds are exceeded. For instance, a vanishing equilibrium may result from predators starving if the prey population drops below a particular threshold. On the other hand, the system stabilizes at a positive balance if prey continues to be plentiful. It was found that Allee effects or high predation pressure can produce bistability conditions in the suggested model. The trivial equilibrium may result from the prey being driven to extinction if the predator population is too high in comparison with the prey. If not, the system might reach a positive equilibrium and stabilize.

Author contributions

Huda Abdul Satar: Investigation, methodology, validation, software, writing-review and editing; Raid Kamel Naji: Data curation, formal analysis, investigation, methodology, software, validation, visualization, writing-original draft, writing-review and editing; Mainul Haque: Formal analysis, investigation, verification, visualization, supervision, writing-original draft, writing-review and editing.

Use of Generative-AI tools declaration

The authors declare they have not used artificial intelligence (AI) tools in the creation of this article.

Conflict of interest

The authors declare that they have no known competing financial interests or personal relationships that could have appeared to influence the work reported in this paper.

References

1. M. Agarwal, V. Singh, Rich dynamics of a food chain model with ratio-dependent type III functional responses, *Int. J. Eng. Sci. Technol.*, **5** (2013), 124–141. http://dx.doi.org/10.4314/ijest.v5i3.10
2. N. Ali, M. Haque, E. Venturino, S. Chakravarty, Dynamics of a three-species ratio-dependent food chain model with intra-specific competition within the top predator, *Comput. Biol. Med.*, **85** (2017), 63–74. https://doi.org/10.1016/j.compbiomed.2017.04.007
3. S. A. Momen, R. K. Naji, The dynamics of Sokol-Howell prey-predator model involving strong Allee effect, *Iraqi J. Sci.*, **62** (2021), 3114–3127. https://doi.org/10.24996/ijs.2021.62.9.27
4. S. A. Momen, R. K. Naji, The dynamics of modified Leslie-Gower predator-prey model under the influence of nonlinear harvesting and fear effect, *Iraqi J. Sci.*, **63** (2022), 259–282. https://doi.org/10.24996/ijs.2022.63.1.27
5. W. M. Alwan, H. A. Satar, The effects of media coverage on the dynamics of disease in prey-predator model, *Iraqi J. Sci.*,**62** (2021), 981–996. https://doi.org/10.24996/ijs.2021.62.3.28

6. P. Cong, M. Fan, X. Zou, Dynamics of a three-species food chain model with fear effect, *Commun. Nonlinear Sci.*, **99** (2021), 105809. https://doi.org/10.1016/j.cnsns.2021.105809
7. S. Debnath, U. Ghosh, S. Sarkar, Global dynamics of a tritrophic food chain model subject to the Allee effects in the prey population with sexually reproductive generalised type top predator, *Comput. Math. Methods*, **2** (2020), e1079. https://doi.org/10.1002/cmm4.1079
8. S. Debnath, P. Majumdar, S. Sarkar, U. Ghosh, Chaotic dynamics of a tri-topic food chain model with Beddington-DeAngelis functional response in presence of fear effect, *Nonlinear Dynam.*, **106** (2021), 2621–2653. https://doi.org/10.1007/s11071-021-06896-0
9. S. Gakkhar, R. K. Naji, Order and chaos in predator to prey ratio-dependent food chain, *Chaos Soliton. Fract*., **18** (2003), 229–239. https://doi.org/10.1016/S0960-0779(02)00642-2
10. Z. M. Hadi, D. K. Bahlool, The effect of alternative resource and refuge on the dynamical behavior of food chain model, *Malays. J. Math. Sci*., **17** (2023), 731–754. https://doi.org/10.47836/MJMS.17.4.13
11. J. Hale, *Ordinary differential equations*, Wiley-Interscience, 1969.
12. M. Haque, N. Ali, S. Chakravarty, Study of a tri-trophic prey-dependent food chain model of interacting populations, *Math. Biosci.*, **246** (2013), 55–71. https://doi.org/10.1016/j.mbs.2013.07.021
13. S. Hsu, T. Hwang, Y. Kuang, Global analysis of the Michaelis-Menten-type ratio-dependent predator-prey system, *J. Math. Biol.*, **42** (2001), 489–506. https://doi.org/10.1007/s002850100079
14. S. Hsu, T. Hwang, Y. Kuang, A ratio-dependent food chain model and its applications to biological control, *Math. Biosci.*, **181** (2003), 55–83. https://doi.org/10.1016/s0025-5564(02)00127-x
15. H. A. Ibrahim, R. K. Naji, Chaos in Beddington-DeAngelis food chain model with fear, *J. Phys. Conf. Ser.*, **1591** (2020), 012082. https://doi.org/10.1088/1742-6596/1591/1/012082
16. B. Kumar, R. K. Sinha, Dynamics of an eco-epidemic model with Allee effect in prey and disease in predator, *Comput. Math. Biophys*., **11** (2023), 16. https://doi.org/10.1515/cmb-2023-0108
17. V. Kumar, N. Kumari, Controlling chaos in three species food chain model with fear effect, *AIMS Math*., **5** (2020), 828–842. https://doi.org/10.3934/math.2020056
18. R. Lavanya, S. Vinoth, K. Sathiyanathan, Z. N. Tabekoueng, P. Hammachukiattikul, R. Vadivel, Dynamical behavior of a delayed holling Type-II predator-prey model with predator cannibalism, *J. Math.*, **2022** (2022), 4071375. https://doi.org/10.1155/2022/4071375
19. F. H. Maghool, R. K. Naji, The dynamics of a Tritrophic Leslie-Gower food-web system with the effect of fear, *J. Appl. Math*., **2021** (2021), 2112814. https://doi.org/10.1155/2021/2112814
20. F. H. Maghool, R. K. Naji, Chaos in the three-species Sokol-Howell food chain system with fear, *Commun. Math. Biol. Neu*., **2022** (2022), 14. https://doi.org/10.28919/cmbn/7056
21. S. Mandal, N. Sk, P. K. Tiwari, R. K. Upadhyay, Chaos and extinction risks of sexually reproductive generalist top predator in a seasonally forced food chain system with Allee effect, *Chaos*, **34** (2024), 063142. https://doi.org/10.1063/5.0212961
22. N. Mukherjee, S. Ghorai, M. Banerjee, Detection of turing patterns in a three species food chain model via amplitude equation, *Commun. Nonlinear Sci.*, **69** (2019), 219–236. https://doi.org/10.1016/j.cnsns.2018.09.023
23. P. Panday, N. Pal, S. Samanta, J. Chattopadhyay, Stability and bifurcation analysis of a three-species food chain model with fear, *Int. J. Bifurcat. Chaos*, **28** (2018), 1850009. https://doi.org/10.1142/s0218127418500098

24. S. Pathak, A. Maiti, G. P. Samanta, Rich dynamics of a food chain model with Hassell-Varley type functional responses, *Appl. Math. Comput.*, **208** (2009), 303–317. https://doi.org/10.1016/j.amc.2008.12.015
25. D. Pattanayak, A. Mishra, S. Dana, N. Bairagi, Bistability in a tri-trophic food chain model: Basin stability perspective, *Chaos*, **31** (2021), 073124. https://doi.org/10.1063/5.0054347
26. L. Perko, *Differential equations and dynamical systems*, Springer Science & Business Media, **7** (2013).
27. S. Rana, S. Bhattacharya, S. Samanta, Complex dynamics of a three-species food chain model with fear and Allee effect, *Int. J. Bifurcat. Chaos*, **32** (2022). https://doi.org/10.1142/s0218127422500845
28. H. A. Satar, H. A. Ibrahim, D. K. Bahlool, On the dynamics of an eco-epidemiological system incorporating a vertically transmitted infectious disease, *Iraqi J. Sci.*, **62** (2021), 1642–1658. https://doi.org/10.24996/ijs.2021.62.5.27
29. H. A. Satar, R. K. Naji, Stability and bifurcation in a prey-predator-scavenger system with Michaelis-Menten type of harvesting function, *Differ. Equat. Dyn. Syst.*, **30** (2022), 933–956. https://doi.org/10.1007/s12591-018-00449-5
30. J. T. Tanner, The stability and the intrinsic growth rates of prey and predator populations, *Ecology*, **56** (1975), 855–867. https://doi.org/10.2307/1936296
31. R. K. Upadhyay, R. K. Naji, Dynamics of a three species food chain model with Crowley-martin type functional response, *Chaos Soliton. Fract.*, **42** (2009), 1337–1346. https://doi.org/10.1016/j.chaos.2009.03.020
32. S. Vinoth, R. Sivasamy, K. Sathiyanathan, G. Rajchakit, P. Hammachukiattikul, R. Vadivel, et al., Dynamical analysis of a delayed food chain model with additive Allee effect, *Adv. Differ. Equ.*, **2021** (2021). https://doi.org/10.1186/s13662-021-03216-z
33. S. Vinoth, R. Vadivel, N. T. Hu, C. S. Chen, N. Gunasekaran, Bifurcation analysis in a harvested modified Leslie-Gower model incorporated with the fear factor and prey refuge, *Mathematics*, **11** (2023), 3118. https://doi.org/10.3390/math11143118
34. S. Vinoth, R. Vadivel, C. Dimplekumar, G. Nallappan, Dynamical complexities and chaos control in a Ricker type predator-prey model with additive Allee effect, *AIMS Math.*, **8** (2023) 22896–22923. https://doi.org/10.3934/math.20231165
35. F. Zhu, R. Yang, Bifurcation in a modified Leslie-Gower model with nonlocal competition and fear effect, *Discrete Cont. Dyn.-B*, **30** (2025), 2865–2893. https://doi.org/10.3934/dcdsb.2024195

AIMS Press